Iraqi Journal of Physics, 2026
https://doi.org/10.30723/ijp.v24i1.1391

Vol.24, No.1, PP. 21-30
P-ISSN: 2070-4003
E-ISSN: 2664-5548

Investigation of the Effect of Zinc-Oxide Nanoparticles on the Structural and Optical Properties of PVDF- PVA Polymer Blend Thin Films

Fatmia H. Mahdi[1*] and Akram N. Al-Shadeedi[1]
[1]*Department of Physics, College of Science, University of Baghdad, Baghdad, Iraq*
[*]Corresponding author: fatima.mahdi2304@sc.uobaghdad.edu.iq

Abstract
The crystal structure, surface morphology, and optical properties of thin films made from a blend of polyvinylidene fluoride (PVDF) and poly (vinyl alcohol) (PVA), which were doped with zinc oxide nanoparticles (ZnO NPs) at weight ratios of 2, 4, 6, and 10 wt%, were investigated using the solution blending method. Undoped and doped PVDF-PVA polymer blend thin films were deposited using the spin-coating technique. The effect of the addition of ZnO NPs to PVDF-PVA polymer blends was investigated using X-ray diffraction (XRD), field-emission scanning electron microscopy (FE-SEM), and UV-Vis spectroscopy to characterize the crystal structure, surface morphology, and optical properties of thin films. XRD results showed that the addition of ZnO NPs made the PVDF-PVA polymer blend less crystalline. FE-SEM images reveal that the size of ZnO NPs ranges from 35 to 125 nm, which aligns with the results obtained from the Scherrer equation. The optical energy band gap of the PVDF-PVA polymer blend decreases as the doping weight ratios of ZnO NPs increase, which is confirmed by the UV-Vis spectroscopy results.

Article Info.

Keywords:
Polymer Blend, ZnO NPs, Energy Band Gap, Doping, Urbach Energy.

Article history:
Received: Oct. 28, 2024
Revised: Jan. 19, 2025
Accepted: Jan.24, 2025
Published:Mar.01, 2026

1. Introduction
Metal oxide nanoparticle-based polymer blends have attracted interest due to their unique characteristics [1]. From the view of outstanding applications, metal oxide nanoparticle-based polymer blends are considered a new promising class of materials. The incorporation of metal-oxide nanoparticles into the polymer blend could enhance its optical, electrical, thermal, and mechanical properties [2]. The resultant nanocomposites are predominantly utilized in various applications, such as sensors, packaging, catalysts, and industry [3-5].

The organic/inorganic nanocomposites are prepared using matrix materials, such as polymers and small-molecule semiconductors incorporated with nanoscale inorganic materials like metals, metal oxides, and carbon-based nanoparticles [6]. Polymers have large molecules and consist of repeating small units called monomers, which have several characteristics: light-weight, flexible, effective-cost, and low-temperature. On the other hand, inorganic materials with nanoscale have unique structural, electrical, and mechanical properties. Adding inorganic nanoscale materials to the polymer matrix results in materials with superior properties compared to the individual components [7].

The polymer blend is composed of two polymers; mixing these polymers leads to the production of a new material with promising properties [8, 9]. One of the most attractive polymers is polyvinylidene fluoride (PVDF), which has a strong piezoelectric effect [10]. PVDF is a kind of semicrystalline polymer characterized by various properties, including high strong dielectric, firmness, chemical stability, thermo-stability, and piezoelectricity [11]. PVDF owns different applications, such as photo-voltaic devices, battery manufacturing, bio-medical, and sensors [11]. Also, polyvinyl alcohol (PVA) is a distinguished polymer with an attractive chemical structure. PVA polymer is semicrystalline and synthetic, which comprises a chain of carbon and group hydroxyl

functional [12]. PVA is characterized by a wide range of properties, such as biodegradability, water-soluble, thermal stability, chemical resistance, and high tensile strength. These characteristics of PVA pave the road for numerous applications in medical, packaging, textile industry, agriculture, adhesives, and sealants [12].

Inorganic nanoparticles are small-dimensional particles composed of inorganic materials, such as metals and metal oxides. Incorporating inorganic nanoparticles into polymer blends has attracted much attention nowadays due to the small size and unique properties of nanoparticles that enhance the characteristics of polymer blends. To incorporate inorganic nanoparticles into a polymer blend, various techniques are used, such as solution blending, in-situ polymerization, and melt compounding. Numerous metal oxide nanoparticles, like ZnO, WO_3, TiO_2, and Fe_2O_3 are incorporated with polymer blend [13]. One of the most promising n-type semiconductors is zinc oxide (ZnO) metal oxide nanoparticles due to their characteristics, such as wide bandgap, high surface area, and bio-compatibility [14]. ZnO nanostructures are incorporated with polymer blends to prepare nanocomposites with significant properties, such as thermal stability, conductivity enhancement, UV shielding, and high dielectric [15].

In this research, we aim to prepare PVDF-PVA polymer blend thin films, doping with various concentrations of Zinc oxide nanoparticles. The solution blending process was used to fill PVDF-PVA polymer blends with un-changeable PVDF and PVA wt% with different ZnO NPs wt%. X-ray diffraction (XRD), Field Emission Scanning Electron Microscopy (FE-SEM), and UV-Vis spectroscopy were used to investigate the characteristics of thin films.

2. Experimental Work

2. 1. Materials

In this work, the polymers PVDF (polyvinylidene fluoride) with $M_w \approx 534000$ and Poly (vinyl alcohol) (PVA) with $M_w \approx 89000$ were used without additional purification (as received). The metal oxide nanoparticles utilized in this work were Zinc-oxide nanoparticles (as received). The solvents used in this work were methanol, ethanol, and acetone for cleaning, and dimethylformamide (DMF) was used for preparation. All materials and solvents were purchased from Merck.

2. 2. Preparation of Un-Doped and Doped Polymer Blend and Thin Films

PVDF-PVA polymer blend was prepared as follows: 0.5 g of PVDF and PVA were dissolved in 20 mL DMF. The resultant solution was stirred for 4 hrs. To incorporate the PVDF-PVA polymer blend with ZnO NPs, 10 mL of DMF was used to dissolve ZnO NPs with (0, 2, 4, 6, and 10 wt%) according to the polymer blend weight. This mixture was stirred to ensure that the NPs were dispersed to obtain a homogenous mixture. Then, it was added directly to the solution of the PVDF-PVA polymer blend. Finally, the entire solution was mixed and stirred at 60 ° C for 3 hrs to ensure the ZnO NPs had dissolved entirely and dispensed in the PVDF-PVA polymer blend.

The resultant solutions of PVDF-PVA doped with ZnO NPs were deposited by the spin coating technique on glass substrates, which were cleaned through several stages. They were sonicated in soapy water for 15 min. then, in deionized (DI) water for 15 min., and finally, in ethanol and acetone solvents for 15 min. After that, the substrates were rinsed in DI water to remove all residuals. Finally, they were dried by blowing nitrogen gas over them.

The parameters utilized to fabricate thin films by the spin coating technique were 2500 rpm rotation speed and 20 sec. rotation time. The thickness of thin films obtained ranged from 200-300 nm.

2. 3. Characterization of Thin Films

The doping effect of ZnO NPs on PVDF-PVA polymer blends thin films was investigated by characterization techniques as follows:

- The thickness of the thin films was examined by atomic force microscopy (AFM) using AFM TT-2.
- The structural properties of thin films were examined by an X-ray diffractometer (PANalytical 'X' Pert Pro) with CuK_{α} (λ=1.54 A^{o}). The diffraction angles utilized to investigate the structural properties (XRD patterns) ranged from 5^{o} to 80^{o}.
- The surface structure of thin films was analyzed and visualized using field emission scanning electron microscopy (FE-SEM) using FESEM-TESCAN.
- The optical properties of thin films were investigated using an SP-8001 UV/Visible Spectrophotometer. The transmittance spectra were examined in the range of 200-800 nm.

3. Results and Discussion

3. 1. Structural Properties

The structural properties of thin films were investigated by examining the XRD patterns of PVDF-PVA polymer blends doped with ZnO NPs. Fig. 1 presents the ZnO NPs XRD pattern that shows nine diffraction peaks at 2θ of 31.7^{o}, 34.4^{o}, 36.2^{o}, 47.5^{o}, 56.6^{o}, 62.9^{o}, 66.4^{o}, 67.93^{o}, and 69.1^{o} regarding the crystal planes reflection of (100), (002), (101), (102), (110), (103), (200), (112), and (201) of the hexagonal wurtzite structure of ZnO NPs [16], respectively.

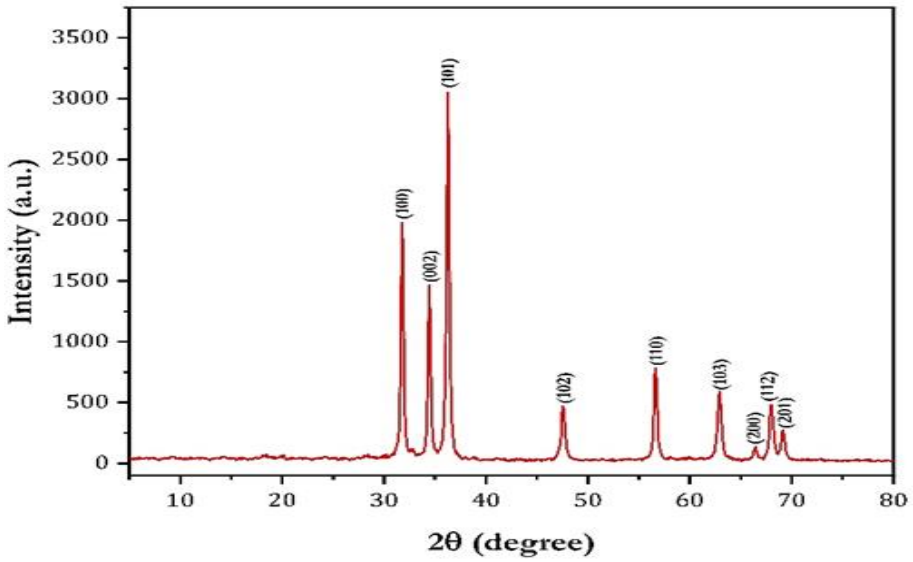

Figure 1: XRD pattern of ZnO NPs.

The average crystalline size of ZnO NPs was calculated by the Scherrer equation, as written in Eq. (1) [17]:

$$D = \frac{k\lambda}{\beta \cos\theta} \quad (1)$$

where D is the crystalline size, k represents a constant with a value of 0.9, the X-ray's wavelength is λ, β is the full width at half maximum (FWHM), and θ is the Bragg angle. The average crystalline size of ZnO NP was found to be 50 nm.

Fig. 2 shows the XRD patterns of PVDF-PVA doped with (0, 2, 4, 6, and 10 wt%) ZnO NPs thin films. The XRD patterns showed peaks at 2θ of 20.25° and a small shoulder at 19.43°. These peaks and small shoulders confirm that the PVDF and PVA were miscible entirely. This result is in good agreement with that of Ismail and Nasr [18]. For the doped PVDF-PVA polymer blend, the ZnO NPs diffraction peaks showed a slight shift towards higher values at 2θ 31.7°, 34.4°, 36.2°, 47.5°, 56.6°, 62.9°, 66.4°, 67.9°, 69.1°. It can be observed that with increased concentration of ZnO NPs, the intensities of diffraction peaks increase, which proves the impact of adding ZnO NPs.

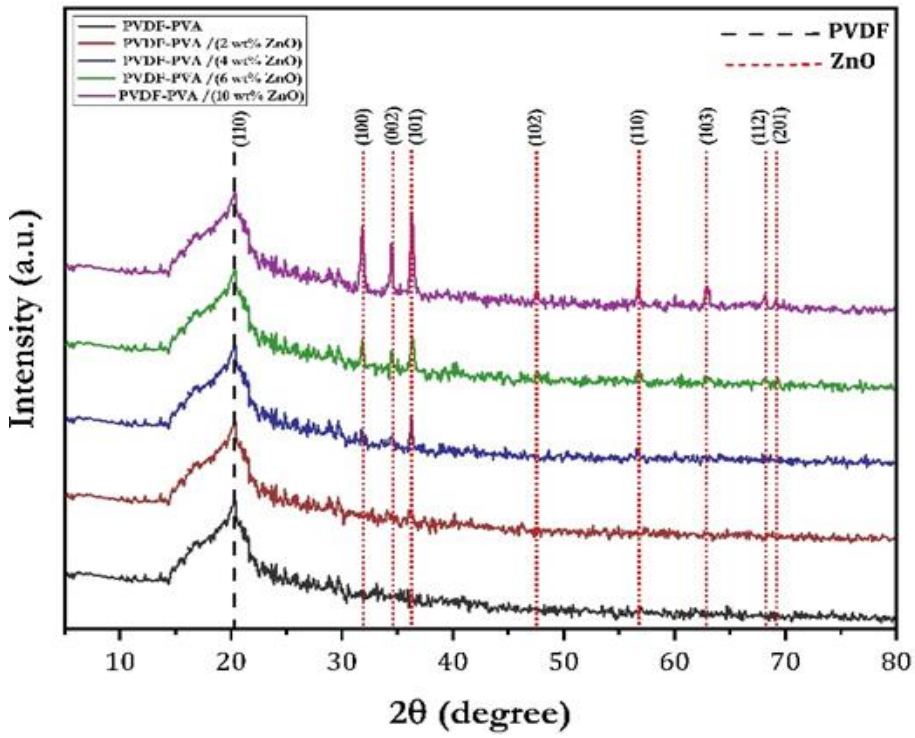

Figure 2: XRD patterns of PVDF-PVA doped with (0,2, 4, 6, and 10) wt% ZnO NPs thin films.

The structural properties of PVDF-PVA doped with ZnO NPs (0, 2, 4, 6, and 10 wt%) thin films can be summarized by the d-spacing (d), dislocation density (δ), and lattice micro-strain (ε), which were calculated by Eqs. (2), (3), and (4), respectively [19, 20]

$$d = \frac{\lambda}{2}\sin\theta \qquad (2)$$

$$\delta = \frac{1}{D^2} \qquad (3)$$

$$\varepsilon = \frac{\beta \cos\theta}{4} \qquad (4)$$

Table 1 lists the structural parameter values for the thin films. The dislocation density and lattice-strain values showed a slight rise as ZnO NPs wt% increased. This attitude generates defects with increasing ZnO NPs concentrations in the PVDF-PVA thin films.

Table 1: Values of structural parameters of PVDF/PVA doped with ZnO NPs thin films.

ZnO wt %	2θ (°)	d (A°)	D (nm)	δ (nm^{-2})	$\varepsilon \times 10^{-3}$
0	20.01	4.42	6.3	0.024	302.5
2	20.12	4.41	6.6	0.022	304.1
4	20.16	4.42	6.5	0.019	304.8
6	20.15	4.38	6.1	0.027	328.6
10	20.2	4.39	7.3	0.025	330.5

3. 2. Field Emission Scanning Electron Microscopy (FE-SEM)

FE-SEM images of the PVDF-PVA doped with ZnO NPs thin films are shown in Fig. 3. FE-SEM image of an un-doped PVDF-PVA polymer blend thin film (Fig. 3(A)) showed a smooth surface with irregular islands. Fig. 3 (B)-(E) shows the FE-SEM images of PVDF-PVA thin films doped with (2, 4, 6, and 10) wt% ZnO NPs illustrating the ZnO NPs doping effect. It can be noticed that the nanoparticles were distributed in the PVDF-PVA polymer blend as spherical dots with sizes ranging from 35-125 nm. These spherical dots agglomerated and increased with increasing ZnO NPs weight ratios.

3. 3. Optical Properties

The absorbance spectra of PVDF-PVA doped with ZnO NPs thin films are presented in Fig. 4. It can be seen that the absorbance spectrum of the PVDF-PVA exhibits a peak at 210 nm, which is related to $\pi - \pi^*$ transition within the polymer chain. The absorbance spectra of PVDF-PVA doped with ZnO NPs thin films show that the absorption peaks shifted toward higher wavelengths (red shift), and their intensities increased due to the increase of ZnO NPs concentration. This behaviour confirms the interaction between the ZnO NPs and matrix (PVDF-PVA).

The optical energy gap is a crucial parameter in studying semiconductor and insulator materials. It represents the minimum energy needed to excite electrons from the valance to the conduction band. The transition from valance to conduction band happens as the incident light interacts with the material's electrons. The optical energy gap of PVDF-PVA thin films doped with ZnO NPs was calculated by Tauc's relation, as mentioned in Eq. (5) [21]:

$$(\alpha h\nu)^{1/n} = B\left(h\nu - E_g\right) \qquad (5)$$

where α is the absorption coefficient is determined by $\alpha = 2.303\ (\frac{A}{d})$, A is the optical absorbance, d is the thickness of the film, B is a constant, hν is the photon energy, E_g is the optical energy gap, and n is a value depending on the transition type, which is an allowed direct transition (n=1/2).

Fig. 5 presents Tauc's plots of undoped and ZnO NPs doped PVDF-PVA generated by plotting $(\alpha h\nu)^2$ versus the incident photon energy $(h\nu)$ to calculate the optical energy gap E_g. From Fig. 5, the optical energy gap value of the undoped PVDF-PVA thin film was found to be 5.281 eV, which agrees with the work of Alghamdi [22]. Doping PVDF-PVA with 2, 4, 6, and 10 wt% of ZnO NPs decreased the optical energy gap to 4.459, 4.403, 4.233, and 4.183, respectively, as listed in Table 2. The reduction in the optical energy gap confirms the interaction between the ZnO NPs and matrix (PVDF-PVA), leading to the generation of structural defects and micro-strains [23]. Thus, the density of localized states will increase in the polymer blends' band gap [24, 25].

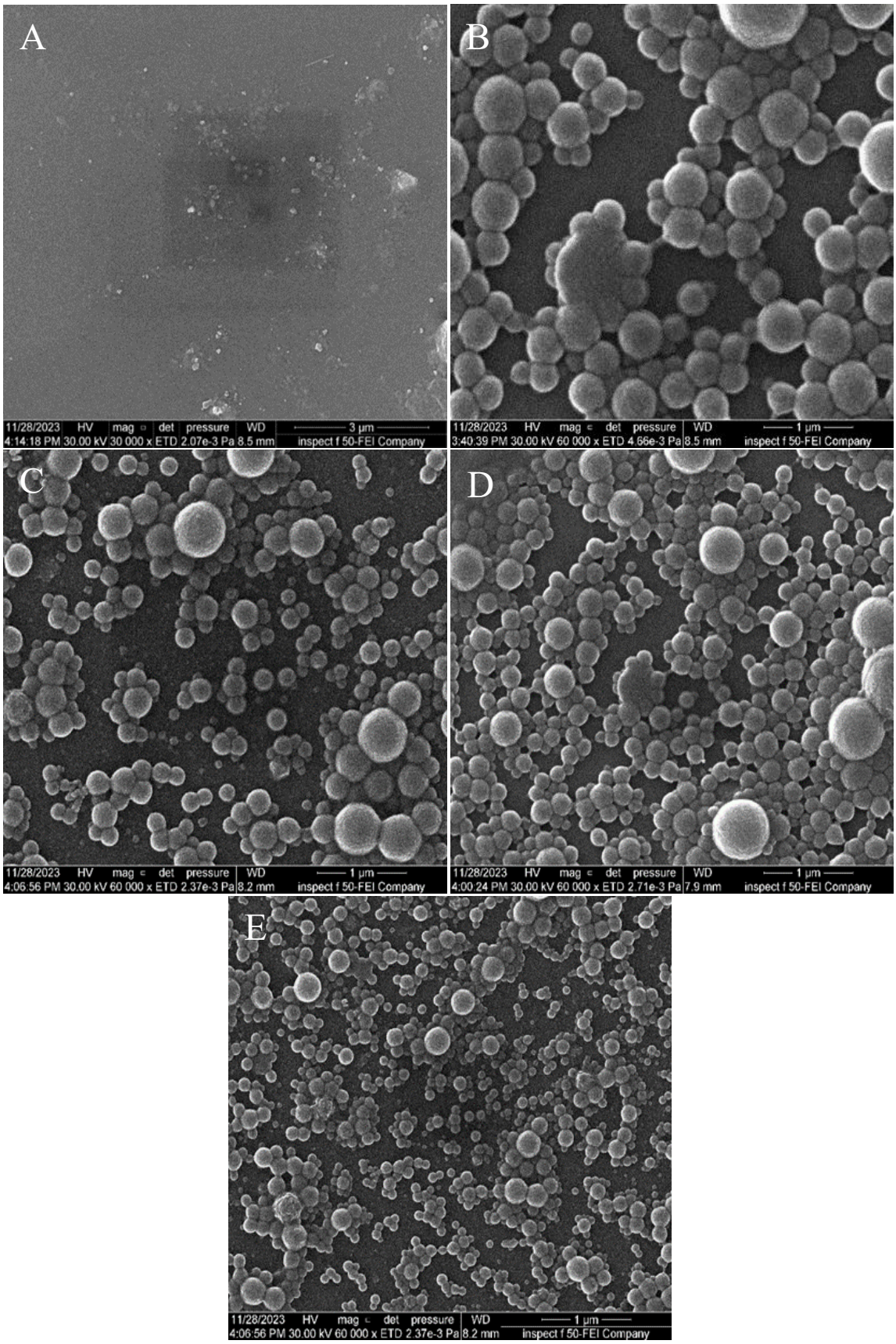

Figure 3: Images of FE-SEM of PVDF-PVA thin films doped with ZnO NPs: (A) 0 wt%, (B) 2 wt%, (C) 4 wt%, (D) 6 wt%, and (E) 10 wt%.

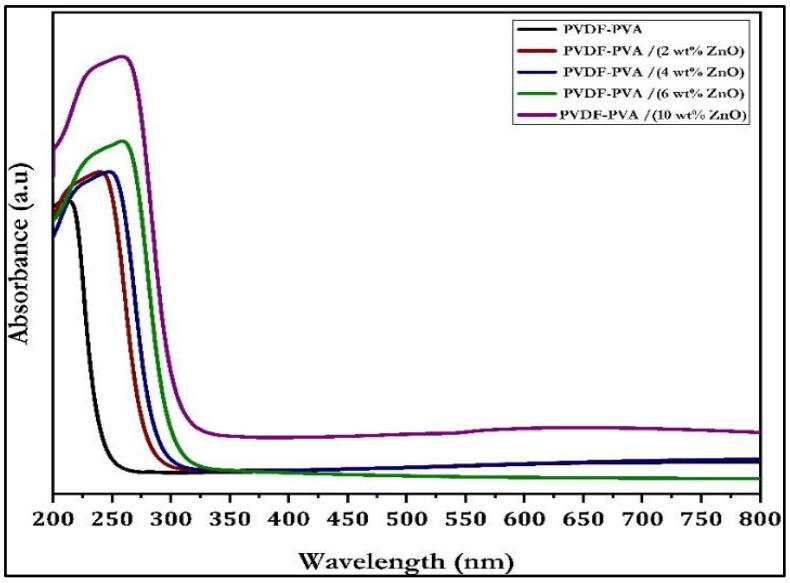

Figure 4: Absorbance spectra of PVDF-PVA thin films doped with (0,2, 4, 6, and 10) wt% ZnO NPs.

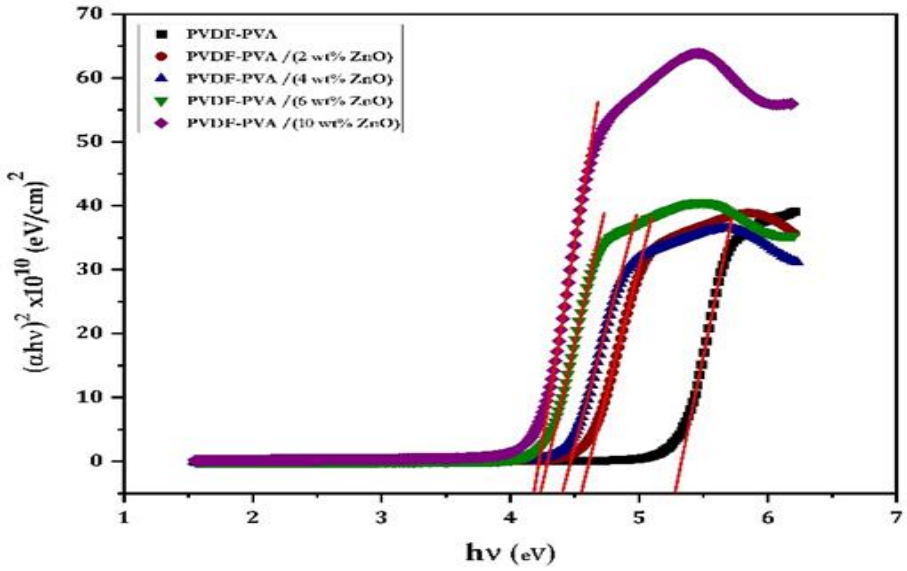

Figure 5: Tauc's plots to extract optical energy gap of PVDF-PVA doped with (0,2, 4, 6, and 10 wt%) of ZnO NPs.

Adding ZnO NPs caused more defects, i.e., increased the density of localized states in the PVDF-PVA. The tail width into the optical band gap of localized states was determined by the Urbach energy model. This model is valid and feasible for determining the shifts that can grow between the extended state at the maximum of the valance band and the localized state at the minimum of the conduction band. Urbach energy can be calculated using Eq. (6) [26]:

$$\alpha = \alpha_o \exp\left(\frac{h\nu}{E_u}\right) \qquad (6)$$

where α_o is a constant, and E_u is the band tail width of localized states into the optical band gap. This relation provides a straight line, and its reciprocal slope represents Urbach energy E_u. As seen in Fig. 6, the values of E_u increased linearly with increasing ZnO NPs concentration compared to that of the undoped PVDF-PVA polymer blend, as listed in Table 2. This behaviour confirms that the density of localized states increases by adding

ZnO NPs to the PVDF-PVA polymer blend due to generating structural defects in PVDF-PVA, leading to high disorder and low crystallinity.

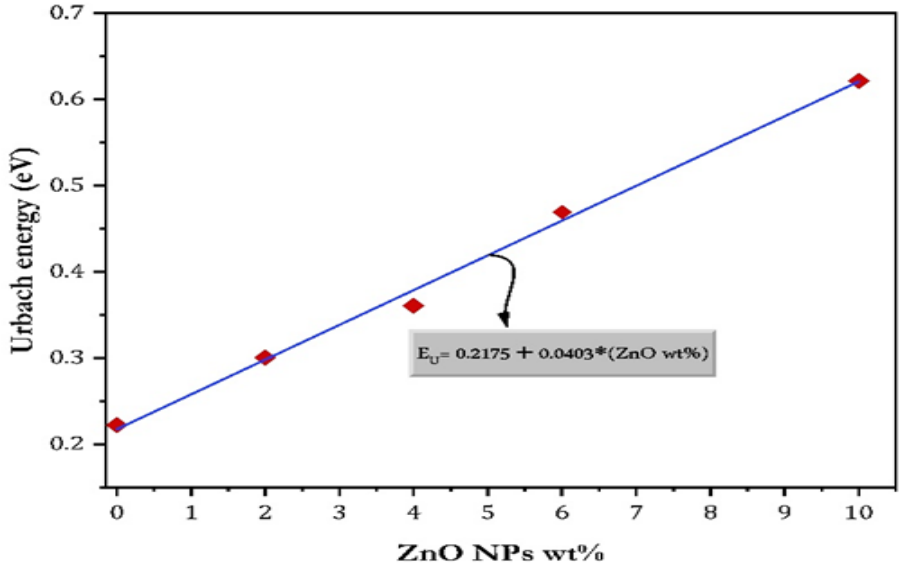

Figure 6: Variation of Urbach energy of PVDF-PVA thin films doped with (0, 2, 4, 6, and 10 wt%) of ZnO NPs.

The impact of the density of localized states is demonstrated in Fig. 7. Fig. 7 presents the exponential decrease in the optical band gap E_g as Urbach energy E_u increases with the addition of ZnO NPs in the PVDF-PVA polymer blend, which means increasing disorder and structural defects in the polymer blend. This result consists of the result of the structural properties.

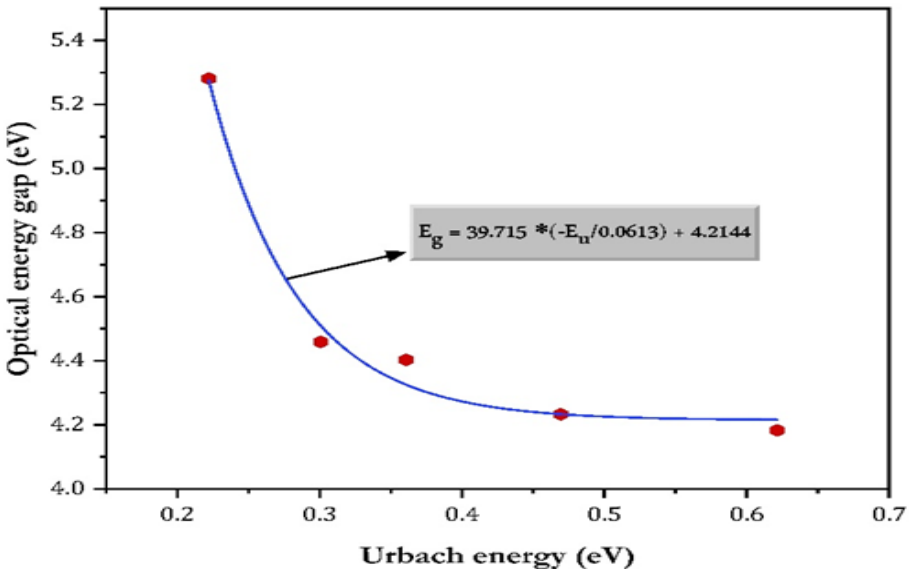

Figure 7: Variation of the optical energy gap versus Urbach energy of PVDF-PVA doped with (0,2, 4, 6, and 10 wt%) of ZnO NPs thin films.

Table 2: Values of optical energy gap and Urbach energy of PVDF-PVA doped with (0,2, 4, 6, and 10 wt%) of ZnO NPs thin films.

ZnO wt %	E_g (eV)	E_u (eV)
0	5.281	0.22227
2	4.459	0.30072
4	4.403	0.36096
6	4.233	0.46932
10	4.183	0.62146

4. Conclusions

PVDF-PVA polymer blend doped with (0,2, 4, 6, and 10 wt%) of ZnO NPs thin films were prepared using the solution blending method. XRD patterns of undoped and ZnO NPs doped PVDF-PVA thin films presented a diffraction peak at 2θ of 20.25°, and a small shoulder at 19.43°, which proves that adding of ZnO NPs decreases the degree of crystallinity of the polymer blend through the results of the crystal structure parameters. The dislocation density of undoped and 10 wt% ZnO doped PVDF-PVA increased slightly from 0.024 to 0.025, respectively, and the lattice strain from 330.5 to 302.5, respectively. FE-SEM images revealed that the average size of ZnO NPs ranged from 35 nm to 125 nm and were distributed as spherical dots. UV-Vis results presented that the absorption peak of PVDF-PVA shifted toward a higher wavelength (red shift) due to the addition of ZnO NPs, which confirms the interaction between the PVDF-PVA and ZnO NPs. The optical energy gap of the un-doped PVDF-PVA polymer blend was 5.281 eV and decreased to 4.183 eV with increasing ZnO NPs doping to 10 wt%. This increase in the optical energy gap is due to the increased localization states in the band gap polymer blend. Also, the Urbach energy of the polymer blend for un-doped and doped with 10 wt% of ZnO NPs increases from 0.222 to 0.621 eV, respectively.

Conflict of Interest

The authors declare that they have no conflict of interest.

References

1. E. Morici, G. Pecoraro, S. C. Carroccio, E. Bruno, P. Scarfato, G. Filippone, and N. T. Dintcheva, Polymers **16**, 922 (2024). https://doi.org/10.3390/polym16070922.
2. A. L. Nikolaeva, A. N. Bugrov, M. P. Sokolova, E. M. Ivan'kova, I. V. Abalov, E. N. Vlasova, and I. V. Gofman, Polymers **14**, 2580 (2022). https://doi.org/10.3390/polym14132580.
3. X. Sun, C. Huang, L. Wang, L. Liang, Y. Cheng, W. Fei, and Y. Li, Adv. Mat. **33**, 2001105 (2021). https://doi.org/10.1002/adma.202001105.
4. S. I. Sharhan and I. M. Ibrahim, Iraqi J. Sci., **60**, 4 (2019). https://doi.org/10.24996/ijs.2019.60.4.9.
5. H. Wu, W. P. Fahy, S. Kim, H. Kim, N. Zhao, L. Pilato, A. Kafi, S. Bateman, and J. H. Koo, Prog. Mat. Sci. **111**, 100638 (2020). https://doi.org/10.1016/j.pmatsci.2020.100638.
6. A. N. Bardan and L. K. Abbas, Iraqi J. Phys. **22**, 1 (2024). https://doi.org/10.30723/ijp.v22i1.1212.
7. H. Shi, J. Chen, G. Li, X. Nie, H. Zhao, P.-K. Wong, and T. An, ACS Appl. Mat. Inter. **5**, 6959 (2013). https://doi.org/10.1021/am401459c.
8. A. K. Khaleel and L. K. Abbas, Optik **272**, 170288 (2023). https://doi.org/10.1016/j.ijleo.2022.170288.
9. S. Thomas, A. R. Ajitha, and M. Jaroszewski, *Polymer Blend Nanocomposites for Energy Storage Applications* (Aluva, Kerala, India, Elsevier, 2023).
10. R. A. Hasson and A. A. Hasan, Iraqi J. Phys. **22**, 19 (2024). https://doi.org/10.30723/ijp.v22i2.1216.
11. P. Saxena and P. Shukla, Adv. Compos. Hybrid. Mat. **4**, 8 (2021). https://doi.org/10.1007/s42114-021-00217-0.
12. Z. W. Abdullah, Y. Dong, I. J. Davies, and S. Barbhuiya, Poly. Plast. Tech. Eng. **56**, 1307 (2017). https://doi.org/10.1080/03602559.2016.1275684.
13. K. Yang, S. Zhang, J. He, and Z. Nie, Nano Today **36**, 101046 (2021). https://doi.org/10.1016/j.nantod.2020.101046.
14. M. M. Abutalib and A. Rajeh, Poly. Test. **91**, 106803 (2020). https://doi.org/10.1016/j.polymertesting.2020.106803.
15. Q. Zhang, C. S. Dandeneau, X. Zhou, and G. Cao, Adv. Mat. **21**, 4087 (2009). https://doi.org/10.1002/adma.200803827.
16. S. Agarwal, L. K. Jangir, K. S. Rathore, M. Kumar, and K. Awasthi, Appl. Phys. A **125**, 553 (2019). https://doi.org/10.1007/s00339-019-2852-x.
17. A. L. Patterson, Phys. Rev. C **56**, 978 (1939). https://doi.org/10.1103/PhysRev.56.978.
18. A. M. Ismail and R. A. Nasr, J. Appl. Poly. Sci. **139**, 51847 (2022). https://doi.org/10.1002/app.51847.
19. M. Jay Chithra, M. Sathya, and K. Pushpanathan, Acta Metall. Sin. (Engl. Lett.) **28**, 394 (2015). https://doi.org/10.1007/s40195-015-0218-8.
20. T. Dayakar, K. Venkateswara Rao, K. Bikshalu, V. Rajendar, and S.-H. Park, Mat. Sci. Eng. C **75**, 1472 (2017). https://doi.org/10.1016/j.msec.2017.02.032.

21. J. Tauc and A. Menth, J. Non Cryst. Sol. **8-10**, 569 (1972). https://doi.org/10.1016/0022-3093(72)90194-9.
22. H. M. Alhusaiki-Alghamdi, Poly. Bull. **80**, 2137 (2023). https://doi.org/10.1007/s00289-022-04167-5.
23. S. Pervaiz, N. Kanwal, S. A. Hussain, M. Saleem, and I. A. Khan, J. Poly. Res. **28**, 309 (2021). https://doi.org/10.1007/s10965-021-02640-9.
24. S. Shukla, N. K. Sharma, and V. Sajal, Opt. Quant. Elect. **48**, 57 (2015). https://doi.org/10.1007/s11082-015-0351-7
25. A. P. Indolia and M. S. Gaur, J. Poly. Res. **20**, 43 (2012). https://doi.org/10.1007/s10965-012-0043-y.
26. T. Skettrup, Phys. Rev. B **18**, 2622 (1978). https://doi.org/10.1103/PhysRevB.18.2622.

دراسة تأثير جسيمات أكسيد الزنك النانوية على الخصائص التركيبية والبصرية لأغشية خلائط بوليمر PVDF-PVA الرقيقة

فاطمة حيدر مهدي[1] و أكرم نوري الشديدي[1]
[1] قسم الفيزياء، كلية العلوم، جامعة بغداد، بغداد، العراق

الخلاصة
تم دراسة البنية البلورية والتشكل السطحي والخواص البصرية لأغشية رقيقة من خليط بوليمر بولي فينيلدين فلوريد (PVDF) وبولي فينيل الكحول (PVA) المضاف إليها نسب وزنية (2، 4، 6، و 10%) من جسيمات أكسيد الزنك النانوية (ZnO NPs) . تم ترسيب الأغشية الرقيقة لخليط البوليمر PVDF-PVA غير المضاف والمضاف إليه ZnO NPs باستخدام تقنية الطلاء الدوراني. تم التحقيق في تأثير إضافة ZnO NPs إلى خلائط البوليمر PVDF-PVA باستخدام حيود الأشعة السينية (XRD) والمجهر الإلكتروني الماسح الانبعاث الميداني (FE-SEM) وطيف الامتصاص فوق البنفسجي- المرئي (UV-Vis) لتوصيف البنية البلورية والتشكل السطحي والخواص البصرية للأغشية الرقيقة. أظهرت نتائج حيود الأشعة السينية (XRD) أن إضافة ZnO NPs يؤدي إلى انخفاض في بلورية خليط البوليمر PVDF-PVA. أظهرت صور المجهر الإلكتروني الماسح الانبعاث الميداني (FE-SEM) أن حجم جسيمات ZnO NPs يتراوح بين 35-125 نانومتر، وهو ما يتفق مع ذلك الذي تم الحصول عليه من معادلة شيرر. انخفضت فجوة الطاقة البصرية لخليط البوليمر PVDF- PVAبزيادة نسب الوزن المضافة منZnO NPs ، وهو ما أكده طيف الامتصاص فوق البنفسجي- المرئي(UV-Vis) .

الكلمات المفتاحية: خليط بوليمر، جسيمات أكسيد الزنك النانوية، فجوة الطاقة، التشويب، طاقة أورباخ.